

## Accepted Manuscript

Title: A G-Quadruplex aptamer based Impedimetric Sensor for Free Lysine and Arginine

Author: Z.A. Carter R. Katakya

PII: S0925-4005(16)31972-4

DOI: <http://dx.doi.org/doi:10.1016/j.snb.2016.12.010>

Reference: SNB 21384

To appear in: *Sensors and Actuators B*

Received date: 5-9-2016

Revised date: 1-12-2016

Accepted date: 2-12-2016



Please cite this article as: Z.A.Carter, R.Katakya, A G-Quadruplex aptamer based Impedimetric Sensor for Free Lysine and Arginine, *Sensors and Actuators B: Chemical* <http://dx.doi.org/10.1016/j.snb.2016.12.010>

This is a PDF file of an unedited manuscript that has been accepted for publication. As a service to our customers we are providing this early version of the manuscript. The manuscript will undergo copyediting, typesetting, and review of the resulting proof before it is published in its final form. Please note that during the production process errors may be discovered which could affect the content, and all legal disclaimers that apply to the journal pertain.

## A G-Quadruplex aptamer based Impedimetric Sensor for Free Lysine and Arginine

Z. A. Carter<sup>a</sup> and R. Katakya<sup>\*a</sup>

Department of Chemistry, University of Durham, South Road, Durham, DH1 3LE, United Kingdom

*E-mail: ritu.katakya@durham.ac.uk*

### Highlights

- 1 A thiolated G-quadruplex aptamer is able to directly detect essential amino acids.
- 2 Amino acids, such as lysine and arginine, can be detected, at picomolar levels of detection, without resorting labelling of amino acids.
- 3 Direct applications in 'real' samples is demonstrated, as proof of concept, using food samples.

### Abstract

This paper describes a label free sensor for the sensitive detection of certain, basic primary amino acids containing free ethyl and methyl amino acids. The control of interfacial electron transfer of a G-quadruplex DNA aptamer, using a  $\text{Fe}(\text{CN})_6^{3-/4-}$  redox probe responds rapidly to variations in arginine and lysine concentrations, but not to histidine, using non-labelled, impedance spectroscopy (EIS) detection. Two binding aptamer binding regimes were observed. At the low concentration range (0-0.15  $\mu\text{g}/\text{ml}$ ), selectivity between lysine and arginine was apparent with limits of detection at approximately 0.5 pM and 1.6 pM, respectively. At higher levels of concentrations, (0.15- 10  $\mu\text{g}/\text{ml}$ ), selectivity was limited. The aptamer was immobilised on gold substrates ensuring optimal probe density which was monitored by Atomic Force Microscopy. Initial studies indicate that the relative change in charge transfer resistance ( $R_{ct}$ ) values can be used as a parameter for monitoring free lysine to arginine ratios and free total lysine and arginine for direct detection of total lysine and arginine in food samples (milk, egg white and yoghurt) in Tris/HCl buffer, demonstrating its potential in many applications.

**Keywords:** G-quadruplex, aptamer, impedance, AFM, amino acids, food

## Introduction

Lysine and arginine are important analytes in clinical diagnostics, biological processes and in the food industry. Lysine cannot be synthesized by mammals and is consequently termed an indispensable amino acid. Recommendations for lysine intake range from 64 to 180 ppm/day, depending on age with an upper limit of 300–400 ppm/day can be considered in humans. A lysine deficiency can lead to a number of health problems including reproductive problems, anaemia and increased recurrence rates of Herpes Simplex attacks<sup>1</sup>. Arginine is classified as a semi essential or conditionally essential amino acid that may be required depending on the health conditions and life cycle of an individual. Preterm infants are unable to synthesize or create arginine internally, making the amino acid nutritionally essential for them. Most healthy people do not need to supplement with arginine because their body produces sufficient amounts. In April 2015, it was reported that arginine breakdown highlighted the early stages of dementia disease in mice<sup>2</sup>. Arginine is also needed to form nitric oxide<sup>3</sup>. Cardiovascular, pulmonary, neurological and intestinal dysfunction can result in preterm infants with a severe deficiency of arginine<sup>4</sup>. Therefore, developing a simple, rapid and accurate detection method for targeting the change in amino acids particularly, in a biological or clinical matrix has important physiological and clinical implications.

Since their discovery in 1990<sup>5,6</sup>, aptamers have attracted intense interest and are receiving further recognition in literature as research reagents, for imaging or diagnostic purposes, and for use in the development of diverse bio-analytical assays<sup>7–13</sup>. Coronary artery bypasses, graft surgery and treatment of proliferative diseases are just some of the procedures that currently utilise aptamers<sup>13</sup>. The high selectivity of aptamers derives from their specific 3D structures, which can distinguish between similar compounds with only subtle structural differences<sup>14</sup>. As an example, in a study by Geiger et al.<sup>15</sup>, an RNA aptamer had an affinity of 0.33  $\mu\text{M}$  to L-arginine and bound  $10^4$  times tighter than to its enantiomer, D-arginine.

Recently several non-labelled aptasensors based on impedance spectroscopy, have been developed. A non-labelled device is reagent-less with no additional molecules covalently bound to the species involved in the binding event<sup>6</sup>. This improves the assay safety as indicators are often toxic, carcinogenic compounds. Wang et al.<sup>16</sup> established the first indicator-free biosensor in 1996. Increased research attention has been given to direct, label-free electrochemical detection formats. By monitoring the changes in an electrical parameter resulting from a target binding or hybridisation event where the aptamer changes conformation, direct detection is feasible which simplifies the protocol.<sup>17</sup> Biomolecules with high target affinity are adopted to ensure a much-improved specificity. This is vital when dealing with complex sample matrices such as cerebral spinal fluid, urine and blood serum<sup>6</sup>. Mei and co-workers<sup>18</sup>, reported an aptamer for binding *p*-nosyl protected alkyl amino group, which they claimed was necessary to circumvent any nonspecific electrostatic interaction of positively charged amino acids at physiological pH with the aptamer. Eissa et al.<sup>19</sup> reported a signal off, label-free impedimetric aptasensor for Okadaic Acid (a biotoxin which accumulates in shellfish) using the  $[\text{Fe}(\text{CN})_6]^{3-/4-}$  redox couple. The aptasensor showed a linear range between 100 pg/mL and 60 ng/mL concentrations with a detection limit of 70 pg/mL. Roushani et al.<sup>20</sup> developed a signal-off biosensor based on aptamer-functionalised AuNPs immobilised on a carbon nanocomposite to detect cocaine. Contreras Jiménez et al.<sup>21</sup> developed a label-free impedimetric aptasensor to detect progesterone with a dissociation constant of approximately 17 nM and detection limit of 0.90

ng/mL. Ghosh Dastider et al.<sup>22</sup> also used impedance-based sensing to rapidly detect Salmonella with a microfluidic device, producing accurate and sensitive results. Özcan et al.<sup>23</sup> detected the parathyroid hormone (detection limit of 10-60 fg/mL), which highlights thyroid conditions including thyroid cancer.

In this work we show that a non-labelled impedimetric method can be used to detect directly the essential aliphatic amino acids, lysine and arginine, in their free form, using a G-quadruplex DNA, EA#14.3 aptamer (Scheme 1). EA#14.3 was reported to have a high affinity for ethanolamine coated magnetic beads and in general for ethyl and methylamine containing molecules<sup>24</sup>. Additionally, the aptamer was tested against a number of amino acids and was reported only able to bind to lysine and arginine, which contain an additional amino group in the side chain. We show that the thiolated aptamer EA#14.3 on a gold substrate can be used as a sensor, without requiring any modification of the amino group as reported previously<sup>18</sup>.

## Experimental

**Equipment:** All electrochemical measurements were performed at ambient temperature in a Faraday cage using a computer controlled Autolab Potentiostat (Metrohm Autolab B.V., Netherlands) and NOVA 1.10 software. The thin-film electrodes used comprised 50:150 nm thick, Ti:Au working (1 mm diameter), reference and counter electrode and were supplied by MicruX Technologies, Oviedo (Asturias), Spain. A drop-cell connector (MicruX) was used for connecting the electrodes to the potentiostat. A small glass tube, with a ground joint (bore diameter 5 mm) was placed over the electrode pads to function as an open-ended beaker. Solutions were purged with nitrogen prior to measurement. Fresh substrates were used for each set of measurements.

A Bruker MultiMode MM8 AFM was used for all AFM measurements. A silicon nitride cantilever with an ultra-fine probe tip, (curvature radius of approximately 10 nm), was used to scan across the sample surface. Scan size was set to 5.00  $\mu\text{m}$  with 512 samples per line, to achieve a high resolution. The dynamic ScanAsyst mode (similar to 'tapping mode'), which uses intelligent algorithms to continuously monitor image quality, was adopted in this study. The mechanical probe (or cantilever) oscillates at well below the resonance frequency, causing minimum sample damage. AFM measurements were used to optimise surface modification procedures. A quartz crystal electrode was used to provide a flat surface.

EQCM measurements were performed using a CHI400A series EQCM module. A quartz crystal with a 6 MHz oscillation frequency was used.

**Materials:** All materials were purchased from Sigma-Aldrich unless otherwise stated. All solutions were prepared with ultrapure water (18.2 M $\Omega$ cm resistivity) sourced from a Sartorius AG Arium Comfort system.

The chemicals, tris(hydroxymethyl)aminomethane (Tris base, >99.9%), potassium ferricyanide (99%), potassium ferrocyanide (99%), dibasic potassium phosphate (ACS reagent,  $\geq$ 98%), monobasic potassium phosphate (ACS, 99%), hydrogen peroxide (27.5%), 6-mercapto-1-hexanol (97%), sulphuric acid (Fisher Chemical, laboratory reagent grade,

>95%), ethanol (laboratory reagent grade, 96%), hydrochloric acid (Fisher scientific, laboratory reagent grade, 36%), L-lysine monohydrochloride (Lancaster, ≥99%), L-arginine monohydrochloride (Fluka, >99.5%), L-histidine (L- $\alpha$ -Amino- $\beta$ -imidazolepropionic acid) (>99%), diamond polish (BASI)65. Other analytes used were egg white, semi-skimmed milk (<2% fat) and vanilla yoghurt (0% fat).

PAGE (polyacrylamide gel electrophoresis) purified 5' thiolated DNA oligonucleotides were ordered from Microsynth (Microsynth AG, Balgach, Switzerland). The 96 mer aptamer sequence (Scheme 1, Figure ESI 1) was re-dispersed in a pH 7.6 20 mM Tris/HCl buffer (with 100 mM NaCl, 2 mM MgCl<sub>2</sub>, 5 mM KCl and 1 mM CaCl<sub>2</sub> added), to produce a 6  $\mu$ M aptamer solution which was kept frozen for storage.

**Substrate preparation:** The following analytical procedure was used for the DNA aptamer immobilization on thin film gold electrodes

**A)** Pre-treatment of bare thin-film electrodes to remove any extraneous residues (cyclic voltammetry in 2  $\mu$ L of 20 mM KCl, between -1.5 V to +1.5 V, scan rate 0.1 V/s, 10 cycles).

**B)** Addition of 0.3  $\mu$ L 0.6  $\mu$ M aptamer solution to the working electrode and application of a +600 mV potential for 15 minutes to immobilize the DNA aptamer on the gold electrode surface through Au-S interaction (forming an ordered SAM).

**C)** Addition of 0.3  $\mu$ L of 1 mM 6-mercapto-1-hexanol (MCH) for 40 minutes to displace any non-specifically adsorbed thiol-ssDNA molecules.

range of 100,000 Hz to 0.1 Hz. Equivalent circuits for Nyquist plot were modelled for time = 0 s.

The sensor preparation and measurement technique is shown schematically in Figure 1. The aptamer concentration and deposition potentials were optimised to achieve the optimal packing density for maximum response.

A similar immobilization procedure was used for fresh EQCM crystals but without pre-treatment. The crystal surface was thoroughly cleaned with a piranha solution, was thoroughly with deionized water and dried under Argon prior to use. The immobilization procedure was monitored using AFM measurements. For measurements the 'TestQCM' procedure (Details in ESI Figure 2) was undertaken and repeated before every test. 2 mL of 10  $\mu$ M amino acid solution in Tris/HCl buffer was added to the modified substrates following stabilisation. A new crystal was used for each amino acid.

The performance of the sensor was evaluated using EIS<sup>25,26</sup>, by monitoring the change in electron transfer resistance ( $R_{ct}$  values) from the [Fe(CN)<sub>6</sub>]<sup>3-/4-</sup> redox couple to the electrode affected by the binding of the aptamer layers to the target amino acid. Impedance measurements were carried out in an equimolar 10 mM K<sub>3</sub>Fe(CN)<sub>6</sub>/10 mM K<sub>4</sub>Fe(CN)<sub>6</sub> solution in Tris/HCl buffer. A 250 mV potential (the formal potential of the [Fe(CN)<sub>6</sub>]<sup>3-/4-</sup> redox couple) was applied over a frequency. Measurements were repeated three times.

## Results and Discussions:

### Aptamer probe function;

EA#14.3 has been reported as an aptamer with a consensus for binding free ethyl and methyl amine containing primary amino acids (scheme 1)<sup>24</sup>. A G-quadruplex, is a nucleic acid sequence, rich in guanine, capable of forming a four-stranded structure through hydrogen bonding (cyclic hydrogen bonding for a G-quartet structure<sup>27,28</sup>). These structures are stabilised by cations such as K<sup>+</sup> and are particularly useful for small molecules analysis in complex samples. The K<sup>+</sup> ion can be used to control the electron transfer properties of the G-quadruplex structure. Pelossof and co-workers recently utilised this feature for controlling electron transfer by pH and K<sup>+</sup> switches.<sup>28</sup>

In this work the 96 unit thiolated G quadruplex DNA aptamer sequence EA# 14.3 (Scheme 1, Figure ESI 1), is used to target specific aliphatic alpha amino acids, lysine, arginine and histidine (Figure ESI 2). Reinemann and co-workers<sup>24</sup>, used affinity elution to assess the binding of the EA#14.3 aptamer immobilised on magnetic beads. The aptamer was reported to form specific intermolecular bonds with amino acids that contain a freely accessible methylamine or ethylamine functional group, in the consensus for binding sequence shown in bold in Scheme 1. In presence of K<sup>+</sup> containing buffer, the aptamer folds into G-quadruplexes. The alpha amino acids, lysine (pKa ~10.5), arginine (pKa ~12.5) and histidine (pKa~6) were tested as targets for the aptamer. The binding of aptamer to their targets occur by a combination of molecular shape complementarities, precise stacking interactions of flat molecules, electrostatic interactions, and in particular by specific hydrogen bondings<sup>30</sup>. It is likely that the strong hydrogen bonding interactions with the consensus indicated in bold of the aptamer EA#14.3 (Scheme 1), are predominant in the *specific* recognition of lysine and arginine. Lysine and Arginine have been reported to be capable of forming approximately 375 and 165 hydrogen bonds with the four DNA bases, whereas histidine forms only 40.<sup>31</sup> Thus contrary to previous reports<sup>18</sup>, that it is necessary to protect the amino groups to prevent nonspecific electrostatic interaction in the binding of G-quadruplexes to compounds containing amino groups, our results show that it is possible target amino acids without the unnecessary complication. Arginine and lysine side chains are both positively charged at pH 7.6. Histidine, although it contains an alpha amino acid group, is partially positively charged at pH 7.6, due to the imidazolium nitrogen and its tautomeric forms. Lysine and arginine are found to bind the aptamer whereas no binding is observed with histidine. Thus histidine acts a control in our measurements.

#### Surface coverage:

For non-labelled impedance techniques, one of the keys to successful implementation of detection is optimal surface probe density. The signal transduction depends on the change in charge transfer resistance,  $R_{ct}$ , on the surface. Electrostatic interactions between the gold surface and the DNA probe molecule have been shown to have a reversible effect on the orientation and immobilisation of probes on the gold. An applied voltage of 0.6 V vs Ag/AgCl, for 15 m, was found to produce very reproducible results for probe coverage and stable films with the G-quadruplex aptamer used in this work.<sup>31</sup> The film height was relatively constant as observed by AFM measurements (Figure 2). If the voltage was taken to > 1.0 V vs Ag/AgCl, desorption was observed, consistent with previous publications.<sup>31</sup> Chronocoulometric measurements, using previously published procedures give a value of roughly  $3.0 \times 10^{-12}$  mole  $\text{cm}^{-2}$ .<sup>32</sup> This method has been applied by several researchers and involves comparative chronocoulometric measurements in the presence and absence of a low ionic strength electrolyte (10 mmol  $\text{dm}^{-3}$  tris-HCl buffer at pH7.4) containing a cationic redox probe  $[\text{Ru}(\text{NH}_3)_6]^{3+}$  which electrostatically binds to the anionic phosphate backbone of the aptamer. The

potential was stepped from -250 to -850 mV vs Ag/AgCl for 500 ms. (ESI, Figure 3 ). EIS and electrochemical measurements were performed with the gold electrodes after immobilization with the aptamer only (ESI, Figure 4) and surface coverage was estimated at approximately 60% , from the change in  $R_{ct}$  values. This surface coverage and packing density gave the maximum signal, which leads us to conclude that unfavourable interactions such as possible cross hybridizations between neighbouring aptamers does not affect the response signal.

Atomic force microscopy (AFM), was used to image the electrode surfaces and to compare the bare electrode surface to the surface with the DNA aptamers and 6-mercaptohexanol immobilised surfaces. Nanoscope 8.15 Analysis was used, as described in the experimental section, to produce 3D images of the electrode surface and the cross section tool was used to measure the height variation across the 5.0  $\mu\text{m}$  square scan. The arithmetic mean of the surface roughness factor was calculated for preparation steps listed above. The bare quartz gold plated electrode had a roughness factor of 0.5 nm which increased to 3.2 nm with DNA immobilised on the substrates, giving a height difference of  $2.7\pm 0.2$  nm, reflecting the average height of the aptamer layer. This value is close to previously reported values (2.3 nm) for thrombin aptamers<sup>31</sup>. (Figure 2).

#### **Electrochemical Impedance Spectroscopy (EIS):**

Electrochemical impedance spectroscopy (EIS) was applied to characterise the binding efficiency of free lysine and arginine to the aptamer by monitoring changes in charge transfer in the presence of the  $\text{Fe}(\text{CN})_6^{3-/4-}$  redox couple. G-quadruplexes are known to be stabilized by cations such as  $\text{K}^+$ , one of the constituents of the buffer used here. The electrostatic repulsion normally exhibited between the negatively charged DNA aptamer probe and the negatively charged  $\text{Fe}(\text{CN})_6^{3-/4-}$  redox couple is partially reduced by the presence of the  $\text{K}^+$  ions. A barrier for the interfacial electron transfer is introduced by conjugation of the amino acids with the aptamer, resulting in a relative increase in the electron transfer resistances. This change in the  $R_{ct}$  value was sufficient to be detected directly without resorting to redox labelling of the aptamer or modifying the amino acid analyte.

Small, precise volumes of 1 mM amino acid in 20 mM Tris/HCl buffer were gradually added to 150  $\mu\text{L}$  of 10 mM  $\text{K}_3\text{Fe}(\text{CN})_6/10$  mM  $\text{K}_4\text{Fe}(\text{CN})_6$  solution to produce varying total concentrations of the amino acid. Concentrations were calculated taking dilution effects into consideration. An increasing resistance to electron transfer ( $R_{ct}$ ) with increasing concentration of amino acid was observed for lysine and arginine (Figures 3a and 3b). Three sets of experiments were performed with fresh electrodes. The response of the aptamer modified electrodes to the target analyte was plotted as normalised  $R_{ct}$  (Figure 3c) by subtracting  $R_{ct}$  for background buffer and dividing by  $R_{ct}$  at saturation concentrations. This method helps to address differences in  $R_{ct}$  values with different sets of Micrux electrodes. Variations in  $R_{ct}$  values by decomposition of ferri/ferrocyanide and the etching of the gold surface by  $\text{CN}^-$  leading to unreliability of EIS measurements using this redox couple has recently been reported by Vogt and co-workers.<sup>33</sup> By using disposable substrates and normalised measurements this issue may be circumvented.<sup>32</sup> The binding event was kinetically faster with arginine compared to lysine. A virtually nil response was obtained with change in  $R_{ct}$  with varying concentrations of histidine as the analyte. This lack of response with histidine under the same conditions of measurements serves as a control and confirms the selectivity of the EA# 14.3 aptamer.

The dissociation constants  $K_d$ , can be calculated using the method reported by Szymanska et al.<sup>34</sup> and Li et al.<sup>35</sup> using the equation  $\Delta R_{CT} = K_a C$ , where  $K_a$  is the association constant of the aptamer obtained from the slope of the regression lines from Figures 3a (ESI Figure 5, Table 1). Two sets of  $K_d$  were obtained for arginine and lysine. Regression analysis at 95% confidence at the low concentration range, (0-0.15  $\mu\text{g/ml}$ ), gives regression coefficients ( $r^2$ ) of 0.98 and 0.99. The  $K_d$  value for lysine was calculated  $32.1 \pm 0.5$  nM, approximately three times the  $K_d$  value for arginine at  $10.5 \pm 0.5$  nM (Table 1). Regression analysis at higher concentrations, (0.15- 10  $\mu\text{g/ml}$ ) gives much  $K_d$  value approximately  $1.6 \pm 0.1$   $\mu\text{M}$  and  $2.5 \pm 0.1$   $\mu\text{M}$  for lysine and arginine respectively. This analyses strongly suggests there are two binding steps for the aptamer. The selectivity between lysine and arginine is evident only at the lower concentration range, with LODs of 0.5 pM and 1.6 pM, respectively. This may be attributable to the fact that number of different binding motifs for lysine and arginine is very limited.<sup>39</sup> At the higher analyte concentration ranges, the selectivity between arginine and lysine is reduced, the regression analysis shows LOD at 1.2 nM and 1.4 nM, respectively. These observed LODs are three decades of concentration lower than previous publications<sup>37, 40</sup> which report LODs at  $\mu\text{M}$  levels of concentrations.

The responses of lysine and histidine to the EA#14.3 aptamer were further verified with QCM studies (ESI Figure 6). The change in frequency response was measured by starting with an aptamer modified quartz-gold surface which was allowed to stabilize and then exposed to the amino acid solution in buffer A change in mass causing a shift in resonance frequency was seen for lysine. With histidine there was no change in frequency confirming previous reports that histidine is not a **target for the aptamer**. Results with arginine, showed an initial very rapid change in mass but results were not reproducible under the conditions used in this experiment and have not been included.

### Application of EIS for lysine detection in food samples

In order to check whether the sensors are capable of direct use in real samples, levels of lysine in some commonly consumed food products were examined as proof of concept. Lysine residues in proteins exist in both free (available) and complexed forms. In the free form, the  $\epsilon$ -amino group is available for usual amine reactions, while in the latter, it is blocked by different types of covalent linkages.<sup>38</sup> It is likely that freely available  $\epsilon$ -amino groups are available for covalent linkages with the aptamer.

In previous work, Bhandare et al.<sup>39</sup> used high performance liquid chromatography (HPLC) in 2010 to determine arginine, lysine and histidine levels in drug substances. The method was found to be accurate and precise, producing a linear trend from the limit of quantification (46  $\mu\text{M}$  for lysine) to 150% amino acid. In 2012, Zhou et al.<sup>37</sup> used a simple but sensitive colorimetric method to detect lysine. The absorbance ratio was linear for lysine concentrations between 1 to 70  $\mu\text{M}$  (limit of detection was 0.8  $\mu\text{M}$ ). However, complicated pre-concentration processes limit these methods, as well as time consuming steps and the need for expensive instruments.

Samples were prepared according to previously published procedures<sup>37,41</sup> briefly, 5 g of yoghurt (0% fat), egg white and semi-skimmed milk (<2% fat) were accurately weighed and homogenized for three minutes. Each sample was diluted with 20 mL of deionised water, filtered using a 0.45  $\mu\text{m}$  filter paper to obtain a clear solution and kept at 37°C for 24 hours. This method of sample preparation

uses the extraction of the basic amino acids in deionised water due to their hydrophilicity.<sup>37,41</sup> 1% of food sample in 20 mM Tris/HCl buffer was tested. Precise volumes of 10% food sample in Tris/HCl were gradually added to 150 $\mu$ L of 10 mM  $K_3Fe(CN)_6$ /  $K_4Fe(CN)_6$  solution to produce varying total concentrations of the food sample for the impedance tests. The sensor surface was rinsed between each addition to wash out any nonspecific binding. A systematic increase in  $R_{ct}$  was observed upon increase in concentration of the food sample (ESI Figure 7). The response time was rapid. A plot on % concentration of the food sample versus the normalised  $R_{ct}$  values, indicate that the thiol-anchored aptamer could provide a bio-sensing platform for sensitive detection of available lysine. Arginine is less likely to interact with the aptamer as it does not contain free  $\epsilon$ -amino acid groups. (Figure 4). The LOD was 0.25% (v/v) food sample in Tris/HCl buffer, with a linear range between 0.25% and 2% concentration of the food sample.

### Conclusions.

Rapid detection of free essential amino acids in food, healthcare, environment both for applications and fundamental research is valuable. This paper has shown that an aptamer which was previously shown to recognise ethyl and methylamine containing molecules<sup>24</sup> can be used in non-labelled impedance sensing using charge transfer resistance as the transduction signal for detecting total and relative ratios of lysine and arginine, at sub-nanomolar levels of concentration. The aptamer modified sensor surface characteristics was optimised and characterised by AFM, EQCM, EIS and electrochemistry. Direct usage in dairy products and egg white were shown as proof of concept for 'real' applications where interactions of freely available lysine residues are likely to interact with the aptamer.

### References

- 1 M. A. McCune, H. O. Perry, S. A. Muller and W. M. O'Fallon, *Cutis*, 1984, **34**, 366–373.
- 2 M. J. Kan, J. E. Lee, J. G. Wilson, A. L. Everhart, C. M. Brown, A. N. Hoofnagle, M. Jansen, M. P. Vitek, M. D. Gunn and C. A. Colton, *J. Neurosci.*, 2015, **35**, 5969–5982.
- 3 FAO/WHO/UNU, *Protein and amino acid requirements in human nutrition*, WHO Press, 2007.
- 4 P. J. Andrew and B. Mayer, *Cardiovasc. Res.*, 1999, **43**, 521–531.
- 5 C. Tuerk and L. Gold, *Science*, 1990, **249**, 505–510.
- 6 A. D. Ellington and J. W. Szostak, *Nature*, 1990, **346**, 818–822.
- 7 B. Deng, Y. Lin, C. Wang, F. Li, Z. Wang, H. Zhang, X. F. Li and X. C. Le, *Anal. Chim. Acta*, 2014, **837**, 1–15.
- 8 M. N. Velasco-Garcia and S. Missailidis, *Gene Ther Mol Biol*, 2009, **13**, 1–10.

- 9 C. L. A. Hamula, J. W. Guthrie, H. Zhang, X. F. Li and X. C. Le, *TrAC - Trends Anal. Chem.*, 2006, **25**, 681–691.
- 10 E. Luzi, M. Minunni, S. Tombelli and M. Mascini, *TrAC Trends Anal. Chem.*, 2003, 810–818.
- 11 A. B. Iliuk, L. Hu and W. A. Tao, *Anal. Chem.*, 2011, **83**, 4440–4452.
- 12 T. Hermann and D. J. Patel, *Science*, 2000, **287**, 820–825.
- 13 M. Khati, *J. Clin. Pathol.*, 2010, **63**, 480–487.
- 14 B. Prieto-Simón, M. Campàs and J. L. Marty, *Bioanal. Rev.*, 2010, **1**, 141–157.
- 15 A. Geiger, P. Burgstaller, H. VonderEltz, A. Roeder and M. Famulok, *Nucleic Acids Res.*, 1996, **24**, 1029–1036.
- 16 J. Wang, X. Cai, B. Tian and H. Shiraishi, *Analyst*, 1996, **121**, 965.
- 17 F. Lucarelli, G. Marrazza, A. P. F. Turner and M. Mascini, *Biosens. Bioelectron.*, 2004, **19**, 515–530.
- 18 H. Mei, T. Bing, X. Yang, C. Qi, T. Chang, X. Liu, Z. Cao, and D. Shangguan., *Anal. Chem.* 2012, **84**, 7323–7329
- 19 S. Eissa, A. Ng, M. Siaj, A. C. Tavares and M. Zourob, *Anal. Chem.*, 2013, **85**, 11794–11801.
- 20 M. Roushani and F. Shahdost-fard, *Anal. Chim. Acta*, 2015, **853**, 214–21.
- 21 G. Contreras Jiménez, S. Eissa, A. Ng, H. Alhadrami, M. Zourob and M. Siaj, *Anal. Chem.*, 2015, **87**, 1075–1082.
- 22 S. Ghosh Dastider, S. Barizuddin, N. S. Yuksek, M. Dweik and M. F. Almasri, *J. Sensors*, 2015, **2015**, 1–8.
- 23 H. M. Özcan and M. K. Sezgintürk, *Biotechnol. Prog.*, 2015, n/a–n/a.
- 24 C. Reinemann, R. Stoltenburg and B. Strehlitz, *Anal. Chem.*, 2009, **81**, 3973–3978.
- 25 D. K. Xu, K. Huang, Z. H. Liu, Y. Q. Liu and L. R. Ma, *Electroanalysis*, 2001, **13**, 882–887.
- 26 M. Nakayama, T. Ihara, K. Nakano and M. Maeda, *Talanta*, 2002, **56**, 857–866.
- 27 J. R. Williamson, *Proc. Natl. Acad. Sci. USA*, 1993, **90**, 3124.
- 28 G. Pelossof, R. Tel-Vered, S. Shimron and I. Willner, *Chem. Sci.*, 2013, **4**, 1137.
- 29 N.M. Luscombe, R.A. Laskowski, J. M. Thornton., *Nucleic Acids Res.*, 2001; **29**(13), 2860–2874.
- 30 T. Hermann and D.J. Patel, *Science*, 2000, **287**, 820–825

31. S.O. Kelley, J. K. Barton, N. M. Jackson, L.D. McPherson. A.B. Potter, E. M. Spain, M. J. Allen, and M. G. Hill., *Langmuir*, Vol. 14, No. 24, 1998, 6781-6784.
32. A. B. Steel, T. M. Herne and M. J. Tarlov, *Anal. Chem.*, 1998, 70, 4670.
33. S.Vogt, Q. Su, C. Gutierrez-Sánchez, and G. Nöll., *Anal. Chem.* 2016, 88, 4383–4390.
34. I. Szymanska, H. Radecka, J. Radecki, R. Kaliszan, *Biosensors and Bioelectronics*, 2007,22, 1955-1960
35. X.Li, L.Shen, D. Zhang, H.Qi, Q. Gao, F.Ma, C. Zhang., *Biosensors and Bioelectronics*, 2008,23, 1624-1630
36. P. Bhandare, P. Madhavan, B. M. Rao and N. Someswar Rao, *J. Chem. Pharm. Res.*, 2010, 2, 580–586.
37. Y. Zhou, Z. Yang and M. Xu, *Anal. Methods*, 2012, 4, 2711.
38. C.C.Goondo, H.E.Swaisgood, G.L.Catignani, *Analytical Biochemistry*, 1981, 115,203-211.
39. H.Hell, N.Sattarahmadt, M.Hajjizadeh, *Anal Methods*, 2014,6,6981-6989.
40. M. Fokkens, T. Schrader, F-G. Klarner., *JACS*, 2005, 127, 14415-14421.
41. J. Wang, P. Zhang, C.M Li ,Y.F YF, C.Z Huang, *Biosensors Bioelectronics.*,2012, 15, 197-201

## Author Biographies

**Ritu Katakya** is Reader (Assoc. Prof), in the department of chemistry at Durham University. Her research interests are in the area of developing hard and soft materials for applications in delivery of actives, implantable/ biocompatible devices and electrochemical sensing. Her work has led to over 110 publications and patents and several international talks. Dr Katakya collaborates extensively with industry. She was past chair of the Electroanalytical Sensing and Systems Group (EAGGG) and has been instrumental in organising several international conferences including, recently, the RSC Analytical Research Forum on Life Sciences and Interfaces, 2012, Faraday Discussion on Nanoelectroanalysis , 2013 and Electrochem 2015.

**Zoe Carter** Zoë Carter graduated in 2015 with a first class honours MSci degree in Natural Sciences (Chemistry and Physics). She is currently training to become a Cardiac Scientist, following the NSHCS Scientist Training Programme at Papworth Hospital. She is also studying a second Masters' in Clinical Science (Cardiac) at Newcastle University. Zoë has great interest in applying scientific research to improve healthcare services, specifically in echocardiography, interventional cardiology and pacemaker devices.

## Figures and Tables

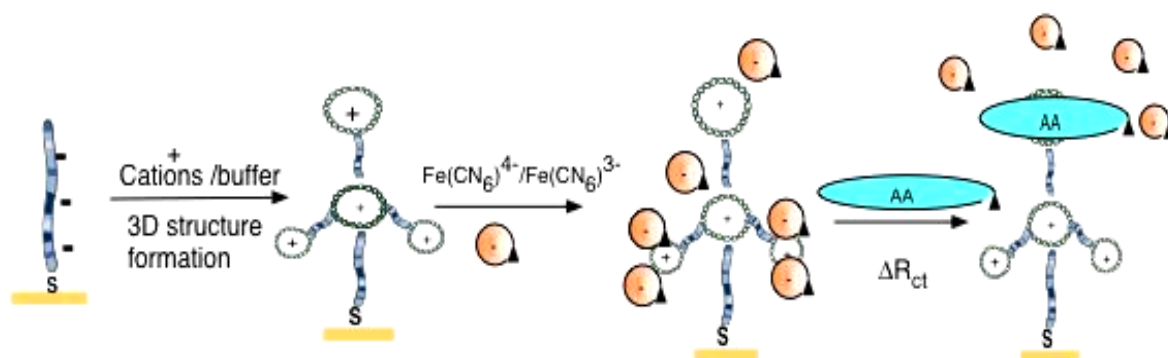


**Figure 1:** Schematic showing the principle underlying direct EIS based measurements, using a DNA G-quadruplex aptamer, which is highly specific for amino acids (AA) that contain a freely accessible methylamine or ethylamine group.

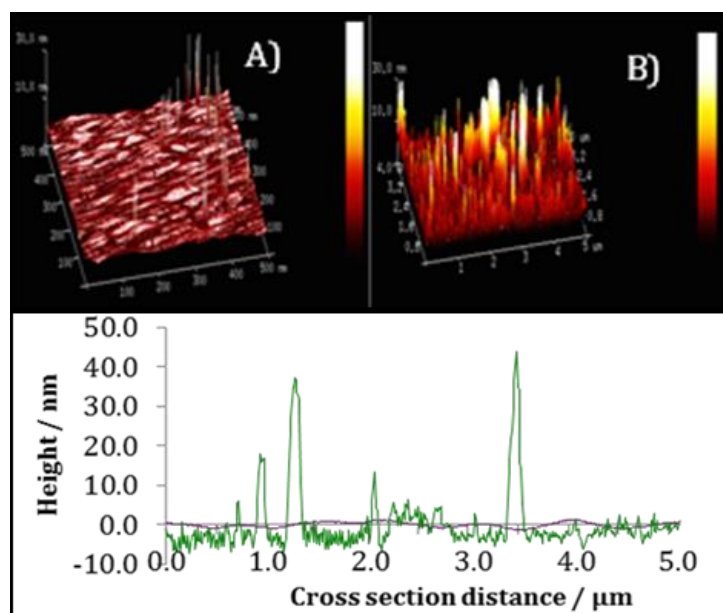


**Figure 2:** AFM 3D images of a gold electrode before (A) and after (B) DNA aptamers and 6 mercaptohexanol immobilization. (C) shows the roughness before (red plot) and after (green plot) surface modification

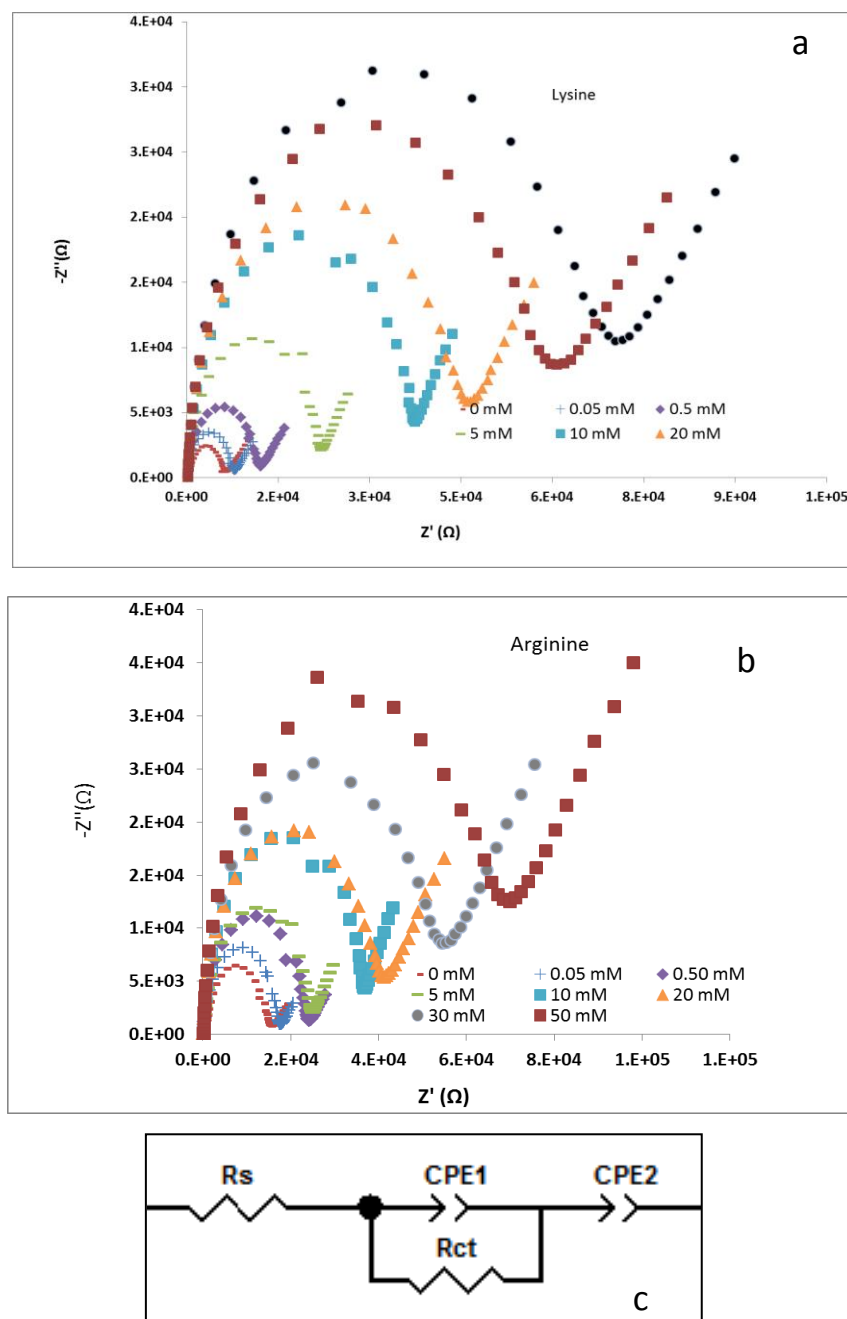


**Figure 3:** Faradaic impedance plots showing change of charge transfer resistance with increasing concentration. (a: lysine, b: arginine, c: model fitted). Measurements were performed in equimolar 10 mM  $K_3Fe(CN)_6$ /10 mM  $K_4Fe(CN)_6$  solution in Tris/HCl buffer. A 250 mV potential was applied over a frequency range of 100,000 Hz to 0.1 Hz.

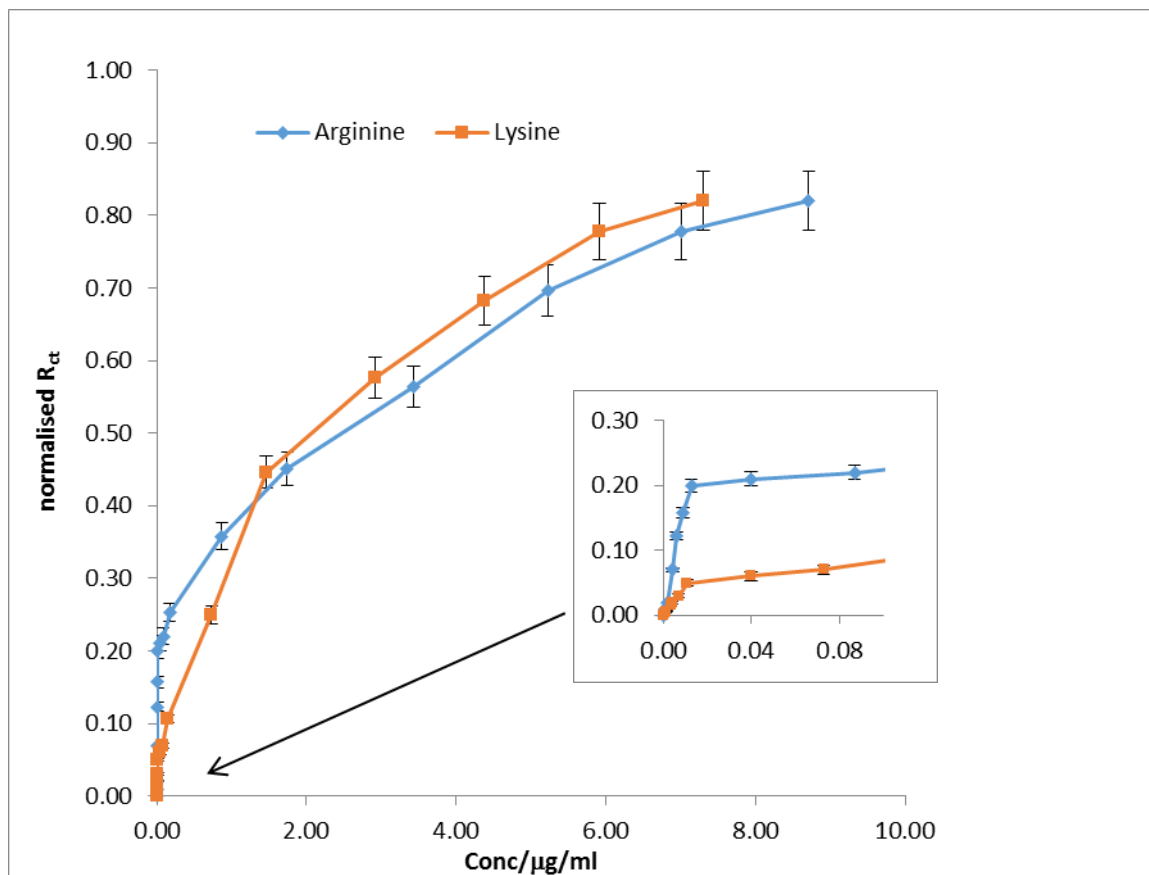


**Figure 3c:** The change in normalised charge transfer resistance with concentration for both lysine and arginine. The inset shows that the differences in normalised  $R_{ct}$  values at low concentrations which may be used for measuring lysine:arginine ratios and total arginine and lysine.

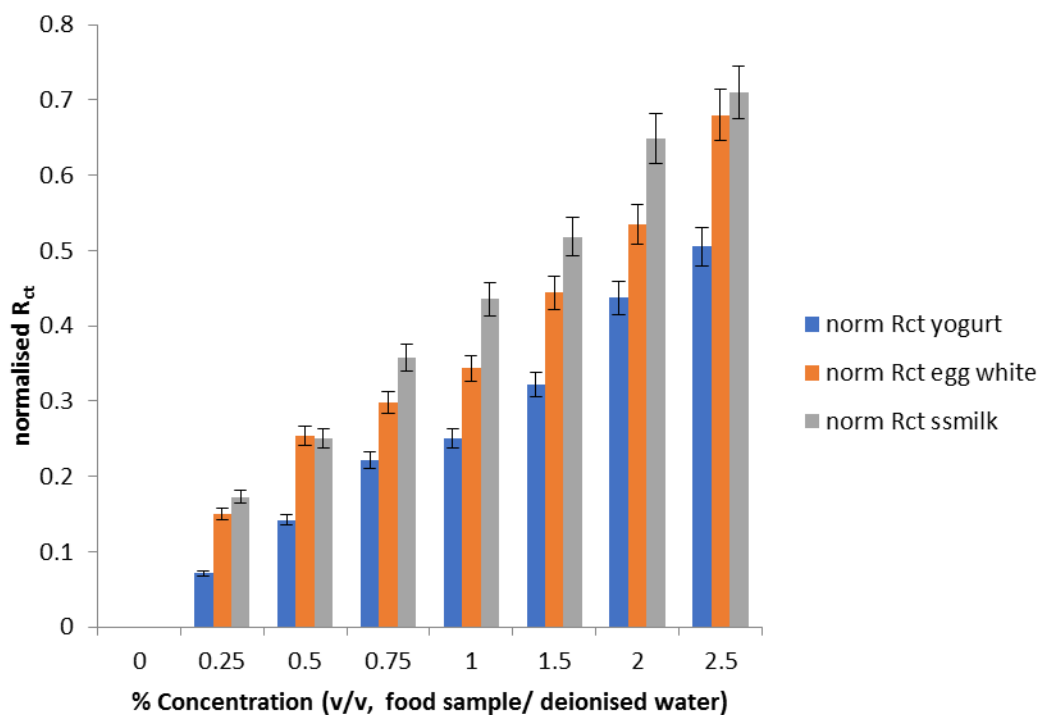


Fig 4: Normalised  $R_{ct}$  values, extracted from Nyquist plots shown in ESI Figure 5 , showing change in response of the aptamer modified electrode surfaces to changes in v/v percent composition of semi skimmed milk (blue), egg white (red) and yogurt (green) .

5'-ATA CCA GCT TAT TCA ATT **TGA GGC GGG TGG GTG GGT**  
TGA ATA CGC TGA TTA CCC CAT CGG AGA ACG TTA AGG CGC  
TTC AGA TAG TAA GTG CAA TCT-3' (**bold** = the consensus  
sequence for binding).

**Scheme 1:** EA#14.3 aptamer sequence used for ethyl and  
methyl amine containing primary amino acid

**Table 1:** Dissociation constant values obtained from regression analyses of the aptamer response from Figure ESI 6

$K_d$	Arginine	Lysine
Low	$10.5 \pm 0.8$ nM	$32.0 \pm 0.1$ nM
High	$2.5 \pm 0.3$ $\mu$ M	$1.6 \pm 0.6$ $\mu$ M